Canadian Conference - Pacific Conference on Earthquake Engineering 2023
Vancouver, British Columbia
June 25th – June 30th, 2023

Semi-active Control of 3D-Vertically Isolated Buildings with Divided Skeleton into Inner and Outer Interactive Subsystems Equipped with MR Dampers

Sasan Babaei[1], Mahmood Hosseini[2*]

[1]PhD Student, Department of Civil Engineering, School of Engineering, Eastern Mediterranean University (EMU), 99628 Famagusta, North Cyprus via Mersin 10, Turkey
[2]Professor, Department of Civil Engineering, School of Engineering, Eastern Mediterranean University (EMU), 99628 Famagusta, North Cyprus via Mersin 10, Turkey, ORCID: 0000-0003-3142-4087
[*]mahmood.hosseini@emu.edu.tr (Corresponding Author)

ABSTRACT

Buildings with vertical seismic isolation, though, benefit from the prominent period shift, and the damping mechanisms placed across the height, are still susceptible to seismic source characteristics. Previous researchers have investigated the effects of subsystems' mass and stiffness ratios, damper type and orientation, as well as hybrid isolation techniques. However, these studies comprise mostly passive dampers and have modeled the lateral load-resisting system in the 2D state. In this study, the semi-active control strategy by using the magnetorheological (MR) dampers was investigated in a 3D state in 6-, 9-, and 12-story buildings, with skeletons divided into two inner and outer subsystems as stiff and flexible parts having dynamic interaction. The lumped mass 3D models of the shear-type buildings were introduced to MATLAB and analyzed subjected to 7 bidirectional ground motions. Inter-story drift, roof relative displacement and absolute acceleration were considered as the seismic responses for evaluation of the buildings' performances. The analyses showed that the passive control, provided by the use of viscous dampers, is only effective in decreasing the stiff subsystem response to nearly half of the uncontrolled building. However, in the soft subsystem, the inter-story drift, on average, is 16 percent greater than the uncontrolled building. This is while by implementing the semi-active control technique by using the MR dampers, the stiff subsystem has a maximum roof displacement, acceleration, and inter-story rotation nearly to 10, 40, and 14 percent of the uncontrolled ones. Furthermore, the average response values of the soft subsystem remained less than half of the uncontrolled system.

Keywords: Vertical isolation, Semi-active control, MR dampers, Performance-based design, Multi-story buildings

INTRODUCTION

Seismic risk reduction of buildings, particularly high-rise structures, is increasingly intertwined with control strategies. Structural damage can be prohibited either by damping the imposed force or shifting the predominant period of the structure. These methods, however, require lateral flexibility at the isolation layer, which can cause large displacement at the base. Common use of a damping mechanism at the isolation level to address this issue, can trigger higher modes in severe earthquakes and make the system less efficient subjected to smaller ground motions. [1, 2]

Hybrid control strategies such as tuned mass dampers and tuned liquid column dampers are also an alternative. Regarding this philosophy, mid-story isolation and sub-system isolation were investigated. This strategy by shifting a portion of the displacement at the base to the upper segment of the building can decrease the displacement at the base. One of the design-based approaches to benefit from a period shift is vertical isolation. In vertical isolation, the lateral load resisting system is divided into two sub-systems, one stiff with less system mass and the other flexible with more system mass. As the system experiences an earthquake, it benefits from the prominent difference between the periods of the two subsystems and the damping mechanisms placed between them across the height. [3-7]

Case sensitivity of passive dampers and the need for a severe power supply and the probability of structural instability in active control have prompted an increase in studies on semi-active control. Semi-active control of MR dampers, although at conventional structures, even adjacent buildings were studied, still vertical isolation was not investigated using semi-active, especially with MR dampers. In this study, the semi-active control strategies by using the magnetorheological dampers were investigated in a 3D state in 6-, 9-, and 12-story buildings, with the skeleton divided into two inner and outer subsystems as stiff and flexible parts. The lumped mass 3D models of the buildings are introduced to MATLAB and subjected to 7 bidirectional ground motions. The passive control of viscous dampers was only effective in reducing the stiff subsystem's response. The semi-active control, however, reduces the maximum roof displacement, acceleration, and interstory drift for both sub-systems for all ground motions, as indicated in the following sections.

SYSTEM DESCRIPTION

In order to portray the dynamic characteristics of the system, lumped mass model at the 3D state was used. In this model, masses are concentrated at sub-systems' floors and each floor of the inner sub-system was joined to that of the outer subsystem by two translational stiffness and damping elements at X and Y directions, and one torsional stiffness and damping element. Each sub-system, therefore, has 3n degrees of freedom (DoF), n DoFs in X and n DoFs in the Y direction and n rotational DoFs. The whole structure has 6n DoFs. Schematic figure of the structure and DoFs of the system at the i^{th} floor are presented in figure 1.

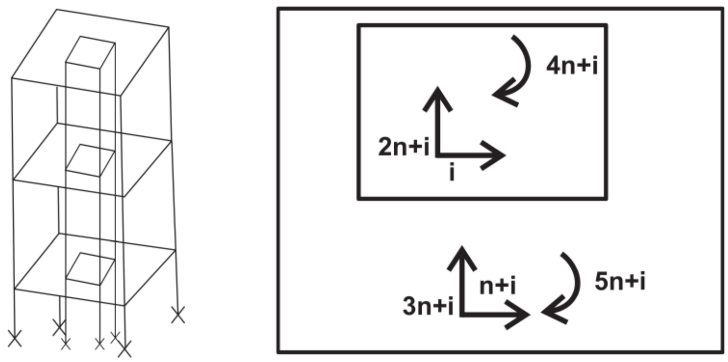

Figure 1. Schematic model of n-story building (left), and DoFs at the i^{th} floor (right)

The matrix form equations of motion of the structural system can be written as:

$$[M_s]\{\ddot{x}(t)\} + [C_s]\{\dot{x}(t)\} + [K_s]\{x(t)\} = [J]\{f_m(t)\} - [M_s][\Lambda]\ddot{x}_g(t) \tag{1}$$

where $[M_s]$, $[K_s]$, and $[C_s]$ are the mass, stiffness and damping matrices of the coupled system, f_m is the MR damper force vector, and $[J]$ is a matrix that defines the location of the control forces. The 6n-DoF mass matrix of the system can be written as:

$$[M_s]_{(6n,6n)} = \begin{bmatrix} m_1 I_n & & & & & \\ & m_2 I_n & & & & \\ & & m_1 I_n & & & \\ & & & m_2 I_n & & \\ & & & & I_{\theta_1} & \\ & & & & & I_{\theta_2} \end{bmatrix} \tag{2}$$

where m_1, and m_2 are the floor masses of the inner and outer sub-systems, respectively, I_n is an identity matrix, and I_{θ_1} and I_{θ_2} are respectively rotational mass matrices of the inner and outer subsystems given by:

$$I_{\theta_1} = I_n . m_1 \frac{(b_1^2 + d_1^2)}{12} \tag{3}$$

$$I_{\theta_2} = I_n . m_1 \frac{(b_2^2 + d_2^2)}{12} \tag{4}$$

The stiffness matrix of the whole 6n-DoF coupled system can be expressed as:

$$[K_s]_{(6n,6n)} = \begin{bmatrix} k_{x_1} & & & & & \\ & k_{x_2} & & & & \\ & & k_{y_1} & & & \\ & & & k_{y_2} & & \\ & & & & k_{\theta_1} & \\ & & & & & k_{\theta_2} \end{bmatrix} + \begin{bmatrix} \begin{bmatrix} k_{d_x} & -k_{d_x} \\ -k_{d_x} & k_{d_x} \end{bmatrix} & & \\ & \begin{bmatrix} k_{d_y} & -k_{d_y} \\ -k_{d_y} & k_{d_y} \end{bmatrix} & \\ & & \begin{bmatrix} k_{d\theta} & -k_{d\theta} \\ -k_{d\theta} & k_{d\theta} \end{bmatrix} \end{bmatrix} \tag{5}$$

In this study, the material of the connectors is considered to remain linearly elastic. [8] Therefore, this matrix is composed of two matrices. The first is the 3-diagonal stiffness matrix of the sub-systems and the second is the effect of the damper placed between the two sub-systems. In this equation, k_1 and k_2 are the results of the mass, frequency ratio, the number of stories in the sub-systems, and the stiffness of the non-isolated building. They can be obtained by coding in MATLAB. $k_{I_{\theta 1}}$ is the torsional stiffness of the system. As it can be seen in the Figure 2, half of the whole system's stiffness for x and y directions is positioned at the floor's center and ¼ of that stiffness is positioned at each of the four sides.

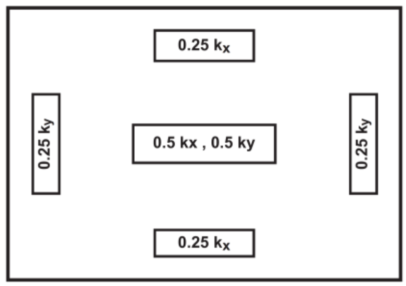

Figure 2. Stiffness distribution of each sub- systems

Torsional stiffness of the sub-system by assuming equal length for floors can be evaluated by the following formulas.

$$k_{x_1} = \begin{bmatrix} K_1 + k_2 & -k_2 & & & \\ -k_2 & K_2 + k_3 & & & \\ & & \ddots & & \\ & & & k_{n-1} & -k_n \\ & & & -k_n & k_n \end{bmatrix} \tag{6}$$

$$k_\theta = 2\left(\frac{1}{4}k_x\frac{d^2}{4} + \frac{1}{4}k_y\frac{b^2}{4}\right) \tag{7}$$

$$k_\theta = k_x\frac{d^2}{4} \tag{8}$$

The k_{d_x} is the systems' damping matrix, expressed in terms of k_{d_i}s (k_{d_i} being the stiffness of the damper at the i^{th} story) as:

$$k_{d_x} = \begin{bmatrix} k_{d_1} & & & \\ & k_{d_2} & & \\ & & k_{d_i} & \\ & & & k_{d_n} \end{bmatrix} \tag{9}$$

For the passive control, the inherent damping is equal to 5 percent, and the viscous damping criteria introduced at FEMA 356 is used to calculate the damping effect between two sub-systems. [9] The damping matrix of C_d can be calculated as:

$$C_d = \begin{bmatrix} C_{c1} & 0 \\ 0 & C_{c2} \\ & \end{bmatrix} \tag{10}$$

The damping coefficients between floors is assumed to be equal and are expressed as:

$$\beta_{1,2} = \frac{\left(\max\{T_{s_1,1}, T_{s_2,1}\}\right) \sum_j c_{cj} (\emptyset_{j,1} - \emptyset_{j,2})^2}{4\pi \sum_i m_i \emptyset_i^2} \tag{11}$$

where $\emptyset_{j,1}$ and $\emptyset_{j,2}$ are the first mode displacement of the two subsystems. $T_{s_1,1}$ and $T_{s_1,2}$ are the first period of the two subsystems, and m_i is the mass of the floor i.

LINEAR QUADRATIC REGULATOR

Linear quadratic regulator (LQR) as a classic, simple and well-known method of optimal control was used in the analyses. In LQR, the control vector should be calculated to minimize the quadratic cost function as:

$$J_{lqr} = \int_0^{\infty} \{x_P(t)^T Q_{lqr} x_P(t) + u_P^T(t) R_{lqr} u_P(t)\} dt \tag{12}$$

where x_P and u_P are the state and the control vectors respectively. The magnitude of decrease in the state variables and the control forces are balanced by weighting matrices Q_{lqr} and R_{lqr}. ρ is the value opted to tune the result which was obtained by trial and error as $\rho = 1 \times 10^{-7.2}$ in this study.

$$Q_{lqr} = \frac{1}{2} \begin{bmatrix} K_s & 0 \\ 0 & M_s \end{bmatrix} \tag{13}$$

$$R_{lqr} = \rho I_{(6n,6n)} \tag{14}$$

NUMERICAL EXAMPLE

In this study, a set of 6-, 9-, and 12-story buildings with the predominant period of 0.6991, 0.9476, and 1.1758, respectively, were modeled in MATLAB. The lumped mass model with the mass placed at the center of the floors was used to model the buildings. Adjacent floors of the sub-systems were connected by the dampers. The floors are rigidly connected by dampers. Any effect of soil on the structure was neglected and the plans of the structures were considered to be symmetric. In order to reduce the analysis time, the state-space was used. Due to sequential environment of the semi- active control, the MATLAB software was used to calculate the control force and displacement at each step. In this study 7 bidirectional records aligned with FEMA P695 provisions was selected and no scaling was introduced. [10]

RESULTS AND DISCUSSION

Roof Displacement Responses

The average maximum roof displacement of the uncontrolled and the passive and semi-active controlled sub-systems are provided at Figure 3. The graph easily portrays that using control, especially semi-active control reduces both inner and outer sub-systems displacements. The soft subsystem, as inherent a long period, gains more displacement for both controls, which is still less than the uncontrolled response.

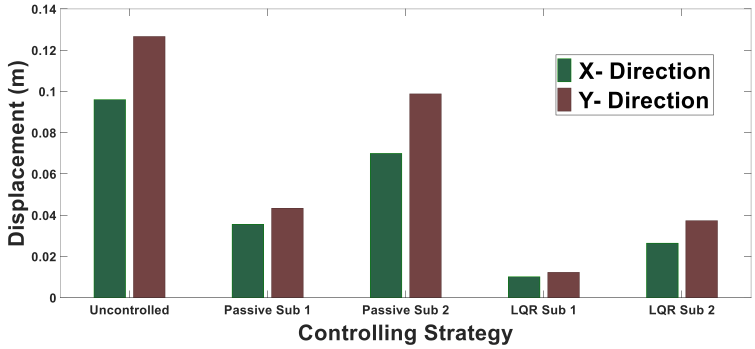

Figure 3. Maximum roof displacement of the sub- systems

At the X direction the passive stiff and soft sub-systems have respectively 0.3705, and 0.7284 of the average roof displacement of the uncontrolled structure. These numbers for the average of 7 records for roof displacements are 0.1056 and 0.2752. In case of passive controlled system these reductions for Y direction are 0.3422 and 0.7803 on average for the 7 considered records. In the semi-active control case, the roof displacement of the two sub-systems are 0.0970, and 0.2949 of the uncontrolled structure. The time history response of Duzce, Turkey, and Manjil Rudbar, Iran earthquakes are presented in Figures 4 and 5.

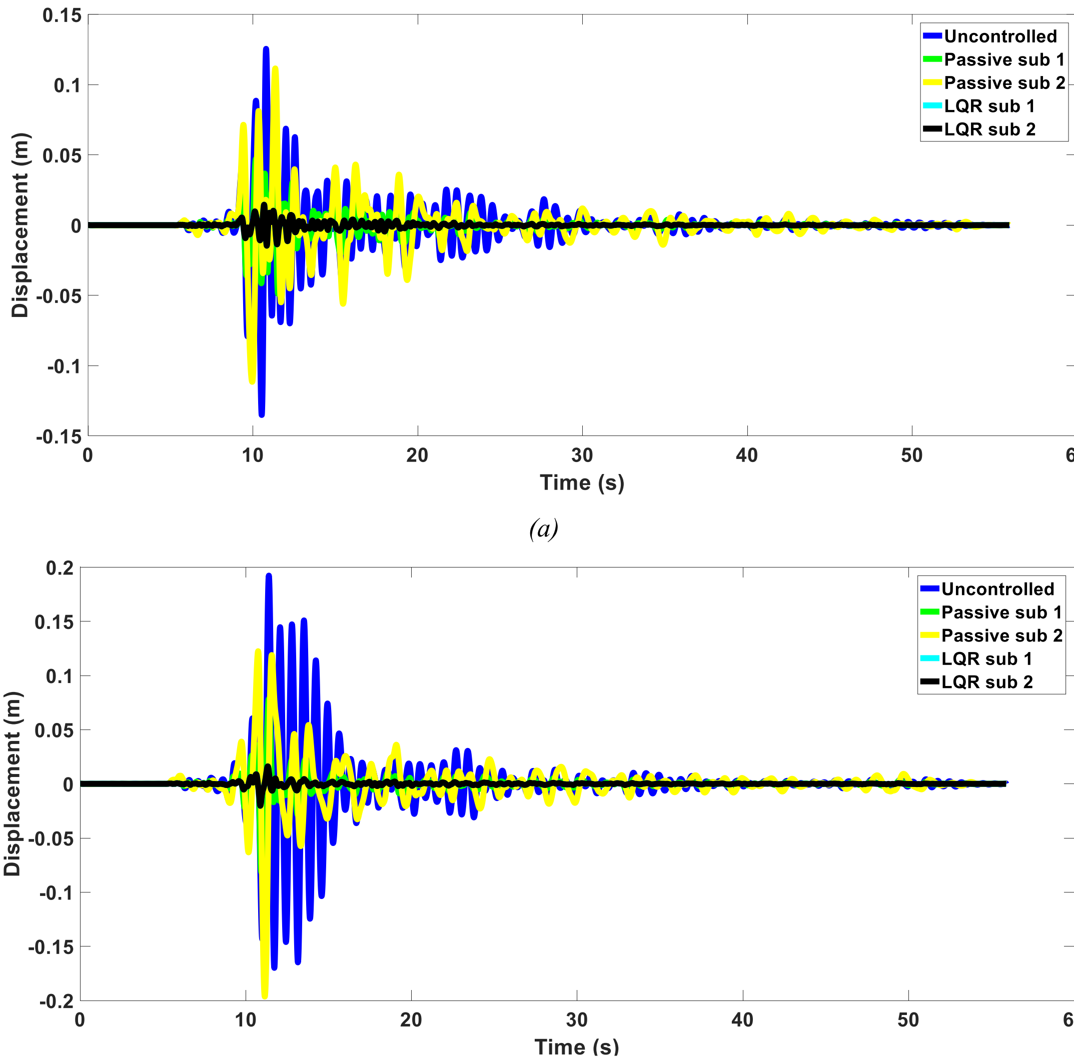

(b)

Figure 4. Roof displacement: a) X dir; b) Y dir subjected to Duzce, Turkey earthquake

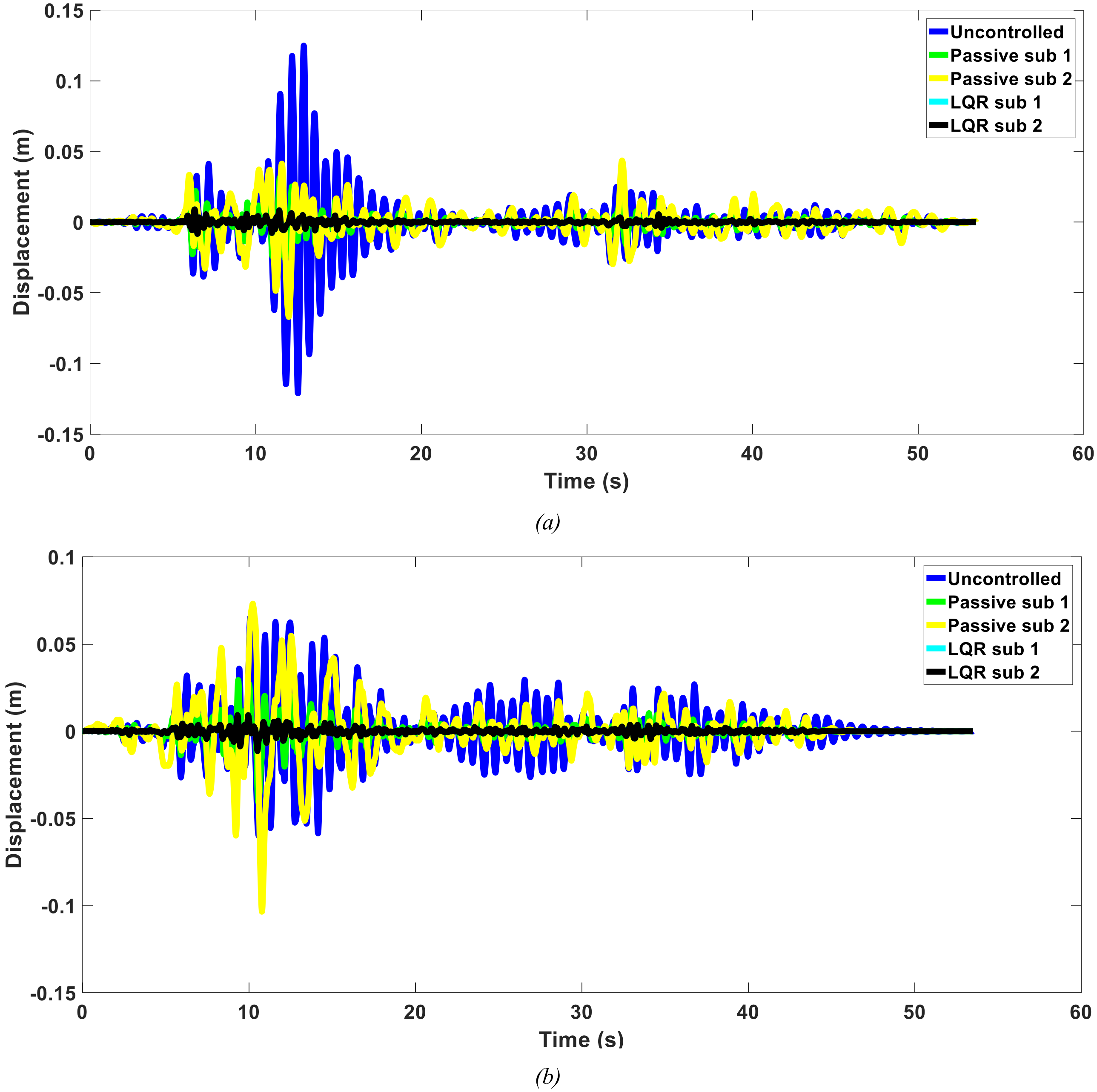

Figure 5. Roof displacement: a) X dir; b) Y dir subjected to Manjil-Rudbar, Iran earthquake

Roof Acceleration Responses

The graphs depict that utilizing a control strategy, especially semi-active control decreases the roof acceleration when subjected to the ground motion. This reduction plays a substantial role to increase the comforts of the residents. The graph also reveals, unlike displacement the stiff and soft sub-systems experience the quite same reduction in their average maximum response for their maximum acceleration at the roof. The ratios of the max average accretion for soft, and stiff sub- structures subjected to the 7 bidirectional records for the passive control are 0.6456, and 0.5531 respectively. This ratios for the semi- actively controlled structure are 0.4057, and 0.3794 respectively. This number for the Y direction reduced more than the X direction which are equal to 0.5739, and 0.5426 for the passive sub-systems. For the semi- actively controlled structure the ratios are 0.3318, and 0.2334 respectively.

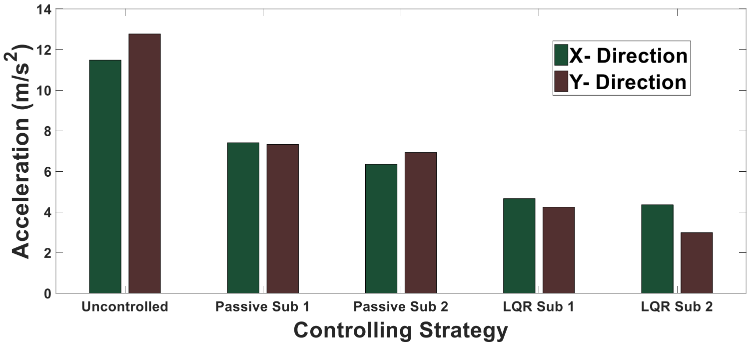

Figure 6. Average max acceleration regarding control and directions

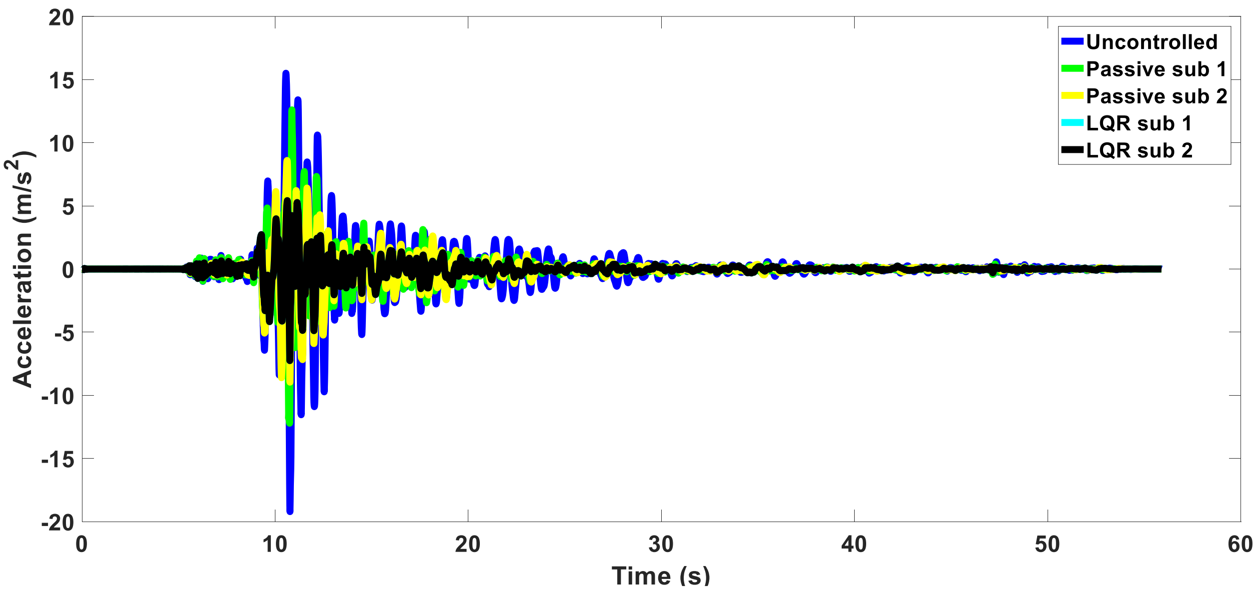

(a)

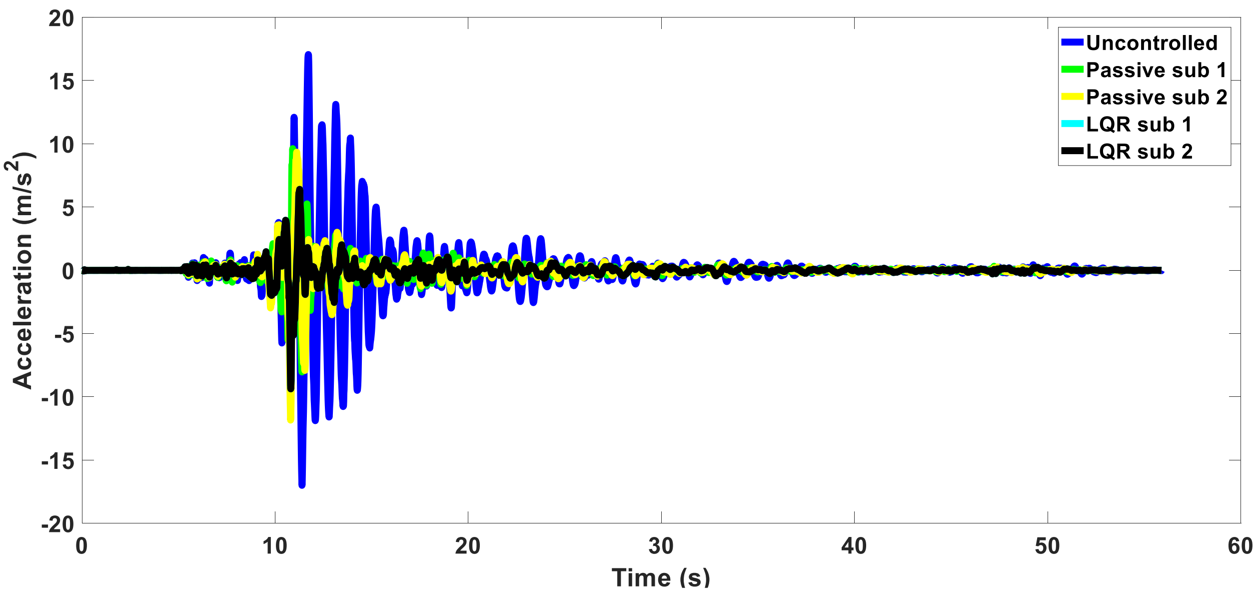

(b)

Figure 7. Roof acceleration: a) X dir; b) Y dir subjected to Duzce, Turkey earthquake

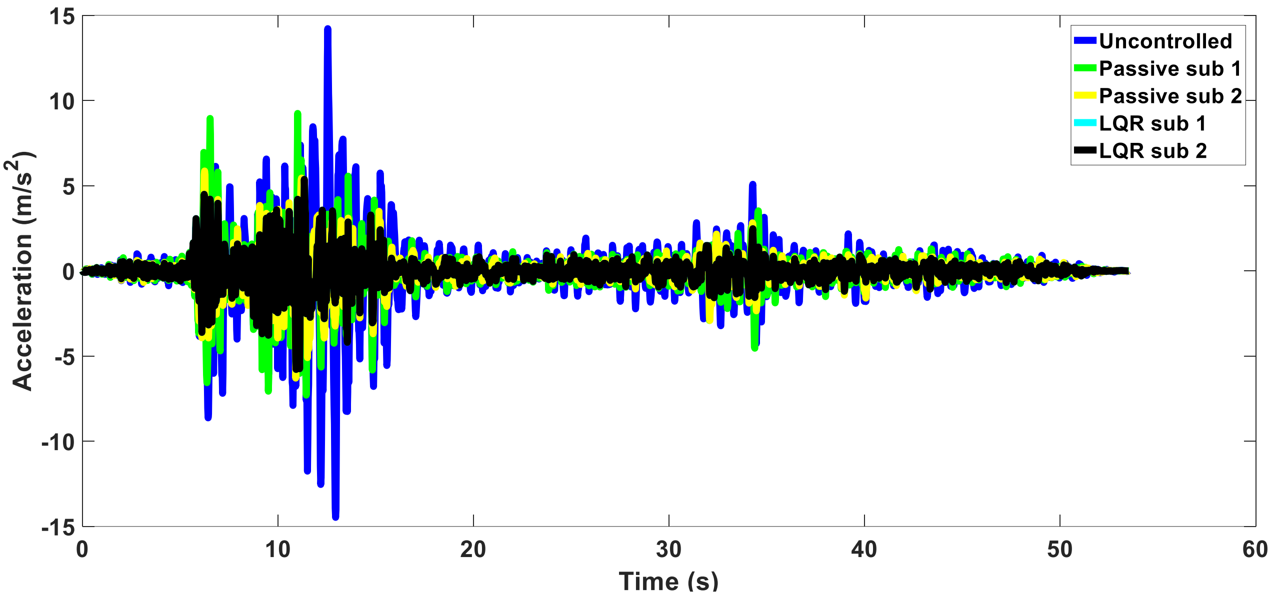

(a)

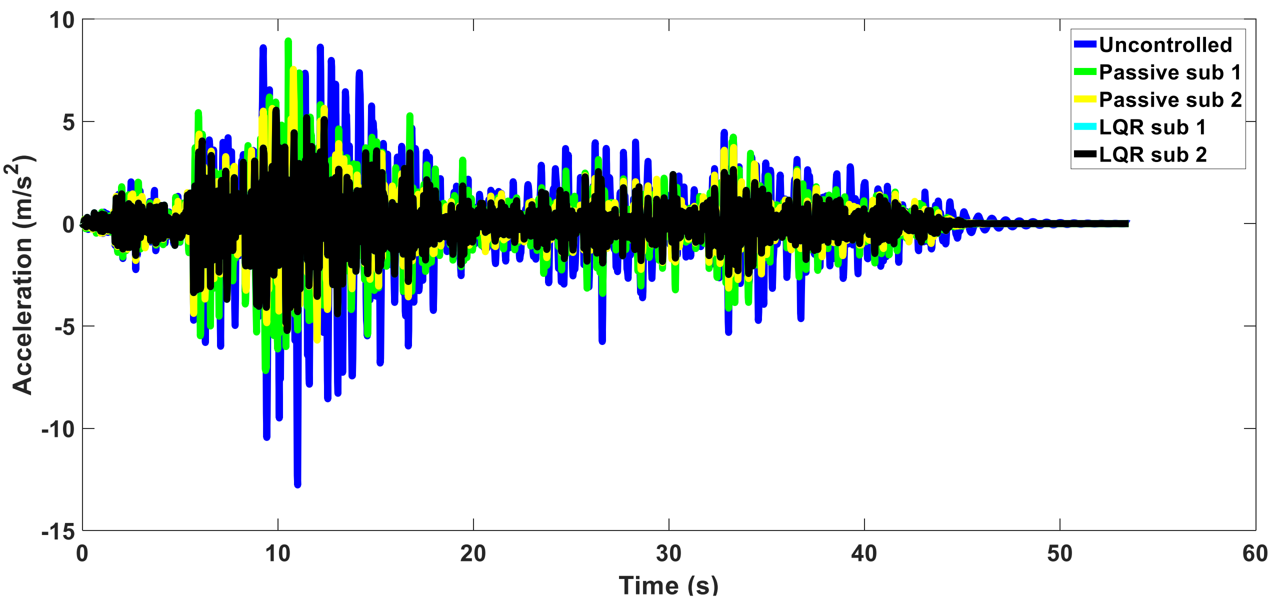

(b)

Figure 8. Roof acceleration: a) X dir; b) Y dir subjected to Manjil-Rudbar, Iran earthquake

Interstory Drift Responses

The other seismic parameter investigated through the analysis was the interstory drift of the uncontrolled and passively and semi-actively controlled structures. Figure 9. easily depicts the passively controlled structure on average for 7 records has the interstory drift ratio of 1.0578, and 0.4522 for its soft and stiff sub-systems. Which for the soft sub-component is a little higher comparing with the uncontrolled one. On the other hand, for the semi-actively controlled sub-system, the ratios for the interstory drifts are 0.4143, and 0.1275 respectively for the two sub-systems. The amount of maximum average interstory rotation for each case also is depicted in the bar chart below.

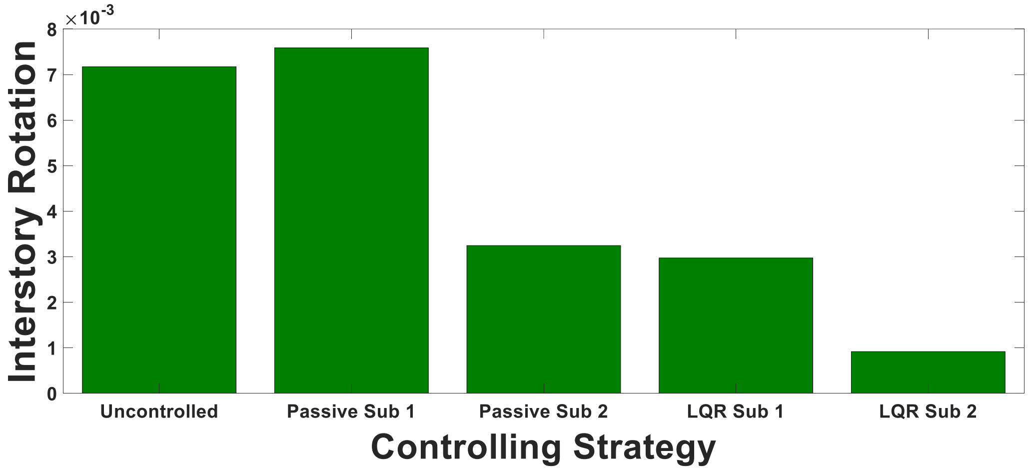

Figure 9. Average max interstory rotation regarding control and directions

The bar chart in figure 6.17 also reveals the soft sub-system at passive control has interstory rotation of 0.76 percent which is greater than the uncontrolled structure with 0.72 percent. The results for the 9 and 12 story buildings are mostly consistence with the 6 story results. The average max roof displacement for the 9 and 12 story are provided in the Figure 10.

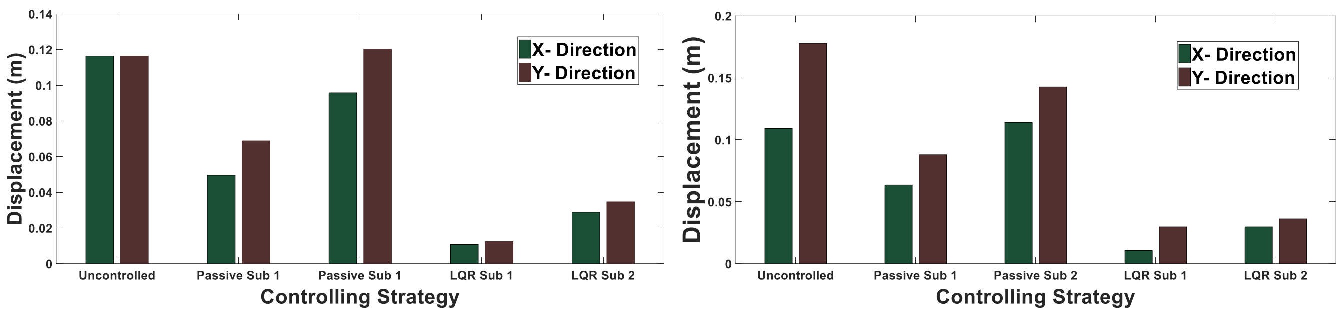

Figure 10. Average max interstory rotation: a) 9story building; b) 12 story building

The max interstory drift for 7 records are also presented at the Figure 11.

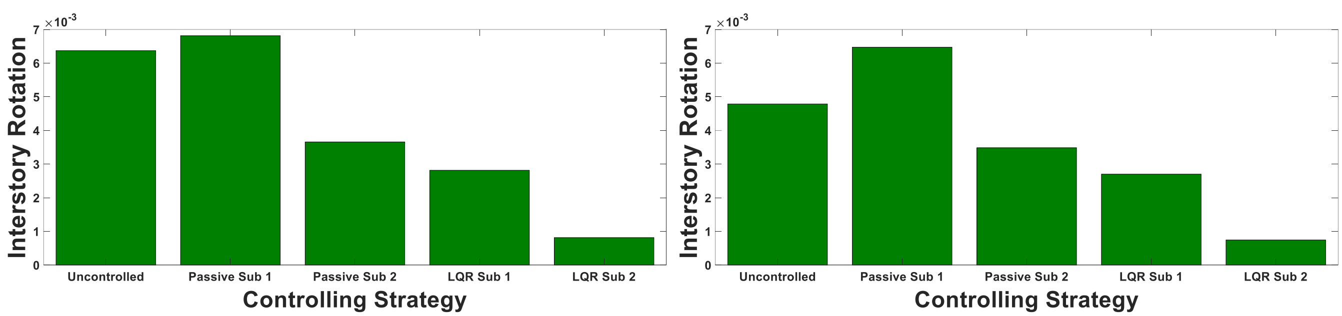

Figure 11. Average max interstory rotation: a) 9 story building; b) 12 story building

CONCLUSIONS

In this study 6-, 9- and 12-story buildings by considering three-dimensional modeling were subjected to 7 bidirectional ground motions. Each structure was investigated without vertical isolation, with passive vertical isolation, and finally with semi-active vertical isolation with an MR damper. The results for all structures delineate that passive vertical isolation can reduce the roof displacement and acceleration for the stiff sub-system. On the other hand, the soft sub-system is sensitive to the selected ground motion. The semi-active control of the structure however was able to reduce sub-system maximum roof displacement, acceleration, and interstory drift. The controlling strategies portrayed prominent response reduction for acceleration even for the passive case. On the other hand, the semi-active strategy is the only control method that reduced the displacement and the interstory drift by greater measures:

- The maximum roof displacement for the 6, 9, and 12- story on average for the inner and outer sub-systems are 46.79 and 86.87 percent of the uncontrolled one. The semi-active control on the other hand reduced displacements to 9.92 and 28.44 percent on average.
- The average maximum roof acceleration of the buildings for the inner and outer sub- systems are 59.33 and 69.35 percent of the uncontrolled one. However, the acceleration as the semi-active control is used dropped to 39.71 and 47.39.
- The average maximum interstory rotation of the sub-systems at 6, 9, and 12-story buildings are 58.5 and 116 percent of the uncontrolled one. The semi-active control was able to decrease it to 13.68, and 47.34.

REFERENCES

[1] M. De Angelis, A. Giaralis, F. Petrini, and D. Pietrosanti, "Optimal tuning and assessment of inertial dampers with grounded inerter for vibration control of seismically excited base-isolated systems," *Engineering Structures,* vol. 196, p. 109250, 2019/10/01/ 2019, doi: https://doi.org/10.1016/j.engstruct.2019.05.091.

[2] D. De Domenico, N. Impollonia, and G. Ricciardi, "Soil-dependent optimum design of a new passive vibration control system combining seismic base isolation with tuned inerter damper," *Soil Dynamics and Earthquake Engineering,* vol. 105, pp. 37-53, 2018/02/01/ 2018, doi: https://doi.org/10.1016/j.soildyn.2017.11.023.

[3] M. Ziyaeifar and H. Noguchi, "Partial mass isolation in tall buildings," *Earthquake Engineering & Structural Dynamics,* vol. 27, no. 1, pp. 49-65, 1998/01/01 1998, doi: 10.1002/(SICI)1096-9845(199801)27:1<49::AID-EQE718>3.0.CO;2-J.

[4] M. Ziyaeifar, "Method of mass isolation in seismic design of structures," in *Twelfth world conference on earthquake engineering*, Auckland, New Zealand, 2000.

[5] R. Milanchian and M. Hosseini, "Study of vertical seismic isolation technique with nonlinear viscous dampers for lateral response reduction," *Journal of Building Engineering,* vol. 23, pp. 144-154, 2019/05/01/ 2019, doi: https://doi.org/10.1016/j.jobe.2019.01.026.

[6] T. C. Becker and A. Ezazi, "Enhanced performance through a dual isolation seismic protection system," *The Structural Design of Tall and Special Buildings,* vol. 25, no. 1, pp. 72-89, 2016/01/01 2016, doi: 10.1002/tal.1229.

[7] M. Nekooei, N. Rahgozar, and N. Rahgozar, "Vertical seismic isolated rocking-core system," *Proceedings of the Institution of Civil Engineers - Structures and Buildings,* vol. 174, no. 8, pp. 627-636, 2021, doi: 10.1680/jstbu.19.00158.

[8] O. A. S. Al-Fahdawi, L. R. Barroso, and R. W. Soares, "Semi-active adaptive control for enhancing the seismic performance of nonlinear coupled buildings with smooth hysteretic behavior," *Engineering Structures,* vol. 191, pp. 536-548, 2019/07/15/ 2019, doi: https://doi.org/10.1016/j.engstruct.2019.04.078.

[9] *FEMA 356 PRESTANDARD AND COMMENTARY FOR THE SEISMIC REHABILITATION OF BUILDINGS*, F. E. M. AGENCY, 2000.

[10] *FEMA P695 Quantification of Building Seismic Performance Factors* FEMA, 2009.